City Research Online

City, University of London Institutional Repository

This is the accepted version of the paper.

This version of the publication may differ from the final published version.

Permanent repository link: http://openaccess.city.ac.uk/id/eprint/22991/

Link to published version: http://dx.doi.org/10.1109/JSEN.2019.2904218

City Research Online: http://openaccess.city.ac.uk/   publications@city.ac.uk

Design and Modeling of a High Sensitivity Fiber Bragg Grating-Based Accelerometer

Qinpeng Liu, Xue He, Xueguang Qiao, Tong Sun, and Kenneth T. V. Grattan

Abstract— Use of a detailed theoretical model has allowed the optimization of the design of a high sensitivity accelerometer, based on a fiber Bragg grating (FBG) and an accelerometer based on this design has been demonstrated experimentally. With a universal model based on double-point encapsulation established, the performance of the device in terms of its optimal sensitivity and frequency distribution has been analyzed, with an optimization 'figure of merit' using the product of the sensitivity and the resonant frequency being presented. The experimental results obtained indicate that the FBG-based accelerometer thus developed shows a broad, flat frequency band, a corresponding flat range sensitivity of ∼152.0pm/G, a resonant frequency of 441.0Hz, and a cross-axis sensitivity of less than 3.6% of the main-axis sensitivity. An accelerometer of this type and with this performance thus has the potential for the important field of low frequency oil-gas seismic exploration.

Index Terms— Fiber Bragg grating (FBG), accelerometer, sensitivity, theoretical model.

I. INTRODUCTION

FIBER Bragg Grating (FBG)-based sensing is an important branch of optical fiber technology and exploits the many advantages of the technology including immunity to electromagnetic interference, high temperature survivability, corrosion resistance, small size and ability to be multiplexed. Sensors of this type can be used to measure many different physical parameters, such as pressure, displacement, angle, and acceleration, suiting them well for important applications in the structural monitoring, geodynamics and seismic exploration fields [1]–[7]. Compared with conventional electronic sensors, the fiber optic approach has unique advantages that suit it well to hazardous measurement situations, such as petroleum exploration where such devices

Q. Liu, X. He, and X. Qiao are with the Key Laboratory on Photoelectric Oil-gas Logging and Detecting, Ministry of Education, School of Science, Xi'an Shiyou University, Xi'an 710072, China (e-mail: lqp1977@163.com; hx_zealot@foxmail.com; xueguangqiao@xsyu.edu.cn).

T. Sun is with the School of Mathematics, Computer Science and Engineering, City, University of London, London EC1V 0HB, U.K. (e-mail:t.sun@city.ac.uk).

K. T. V. Grattan is with the City Graduate School and the School of Mathematics, Computer Science and Engineering, City, University of London, London EC1V 0HB, U.K. (e-mail: k.t.v.grattan@city.ac.uk).

can be used to monitor seismic signals (e.g. which typically occur in the 1–160Hz region). The requirements for such a FBG accelerometer is sensitivity to the appropriate resonant frequencies (showing high sensitivity across a suitable frequency range), limited or zero cross-sensitivity to other key parameters, and a good dynamic and acceleration range, for example. Many different designs of accelerometer based on using highly versatile FBGs have been proposed, and for those based on elastic structures, they can be classified as cantilever structures [8]–[16], tube or cylinder structures [17]–[22], elastic diaphragms [23]–[27] or specialty types of elastic structure [28], [29]. The encapsulation process for the FBG itself can be done through either double-point encapsulation or embedded encapsulation, for example. An FBG-based accelerometer using an elastic cantilever structure can be designed with the design focus being on improving sensitivity to give it maximum utility for the applications area discussed. Classical single cantilever structures have been extensively researched [8]–[14], but typically the frequency bandwidth achieved is very narrow and the cross-sensitivity to other key parameters is very difficult to reduce. In order to create the important and desired reduction of the cross-sensitivity, in practice multiple cantilevers structures have been proposed [15], [16]. Compared with an accelerometer design based on a single cantilever, the elastic tube or cylindrical structure approach has an inherent advantage, in that the axial stiffness of the device is easy to control. Such a structure, combined double-point encapsulation, can be used to improve the sensitivity. Examples of successful designs reported in the literature and which form the background to this work and are considered below. Yu *et al.* [17] have proposed a cylindrical FBG-based accelerometer design with a sensitivity of 80pm/G and resonant frequency of 388Hz. Liu *et al.* [18] proposed an elastic tube-based accelerometer using an FBG, showing a sensitivity of 63pm/G and resonant frequency of 376Hz. Wang *et al.* [19] have proposed a miniaturized FBG accelerometer based on a shell design where the sensitivity achieved is 54pm/G and the resonant frequency 480Hz. In the work of Zhang *et al.* [20], a compliant cylinder accelerometer was discussed where the sensitivity reported was 42.7pm/G and the resonant frequency 400Hz. Gutiérrea *et al.* [21] have presented a cylinder-based FBG accelerometer giving a sensitivity of 19.65pm/G and resonant frequency in excess of 500Hz. Further, Wang *et al.* [22] designed a high frequency accelerometer where the resonant frequency was given as 3806Hz and the sensitivity ∼4pm/G. In general, FBG

accelerometers based on the use of an elastic diaphragm have the useful characteristic of higher sensitivity to the normal displacement but relatively insensitivity to lateral displacement. This benefit then helps to reduce cross-sensitivity to lateral displacement effects, which is important in practical use. Muller *et al.* [23] have proposed a theoretical approach to modeling an accelerometer using double diaphragms. Li *et al.* [24] also presented a FBG accelerometer design based on the double diaphragms, quoting a sensitivity of 24.3pm/G and resonant frequency of 900Hz. Additionally, Luo *et al.* [25] have developed a further FBG accelerometer approach in which the resonant frequency is 143Hz and the sensitivity 211pm/G. Liu *et al.* [26] have also reported an innovative FBG scheme using a single diaphragm, with sensitivity of 36.6 pm/G and resonance frequency of 255 Hz. Important here is that the cross-axis sensitivity is less than 1.3 % of the main-axis sensitivity. Liu *et al.* [27] has developed a device showing a large frequency range and high sensitivity, where the reported sensitivity is 23.8pm/G, the resonant frequency is 1240Hz, and the cross-sensitivity is less than 2.1%.

Balancing the key performance characteristics of sensitivity and resonant frequency is difficult but important to create suitable criteria for achieving optimum performance and allowing cross-comparison with different, competing devices to meet particular operational systems requirements. In this work, the theoretical underpinning of an enhanced FBG-based accelerometer is discussed, thus establishing and an approach to optimization of the performance of FBG-based accelerometer devices. Here the product of the sensitivity and the resonant frequency (PSRF) is introduced as a 'figure of merit' to allow easier comparison and thus optimization of the overall performance, allowing an optimum design for the important frequency range of 1–160Hz to be proposed. Referencing previous work, it can thus be seen when this PSRF 'figure of merit' reaches its optimum value and the sensitivity reaches its maximum within a given frequency band, allowing the design of a sensor to be more compact and thus simpler in operation. This analysis approach is thus well suited to the identification of device designs which show good performance in the low frequency range, making them well-tailored to oil and gas seismic exploration.

II. MODELING AND DESIGN OPTIMIZATION

A. The Theoretical Model Used

The theoretical model used in this work of an FBG-based accelerometer using double-point encapsulation is shown in Fig. 1. In essence, the model can be simplified into a single degree of freedom, mass-spring system, where K is the stiffness of the system, and C is the damping constant. According to coupled-mode theory, the center wavelength shift $\Delta\lambda_B$ of the FBG can be expressed as follows [30]:

$$\frac{\Delta\lambda_B}{\lambda_B} = (1 - P_e)\varepsilon \tag{1}$$

where P_e is the effective elasto-optical coefficient and ε is the axial strain on the FBG. According to the principles of elastic and structural mechanics, the Eq.1 can be
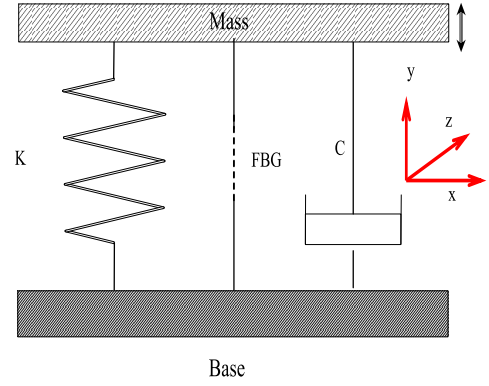

Fig. 1. Simple theoretical model of FBG accelerometer: K is stiffness of system, C is the damping constant and the Fiber Bragg Grating is represented by FBG.

expressed as [19], [27]

$$\frac{\Delta\lambda_B}{\lambda_B} = \frac{(1 - p_e)Ma}{L_f(K_f + K_s)\sqrt{(1 - \gamma^2)^2 + (2\xi\gamma)^2}} \tag{2}$$

where L_f is the length of the fiber used, $K_f = E_f d^2/4L_f$ is its stiffness, K_s is the stiffness of the accelerometer structure, $\gamma = f/f_n$ is the ratio of the frequency to the resonant frequency, ξ is the damping ratio and M is the mass of the inertial system. From the definition of the acceleration sensitivity and the resonant frequency, the sensitivity S_f and the resonant frequency f_n can be expressed as

$$f_n = \frac{1}{2\pi}\sqrt{\frac{K_s + K_f}{M}} \tag{3}$$

$$S_f = \frac{(1 - p_e)M\lambda_B}{L_f(K_f + K_s)\sqrt{(1 - \gamma^2)^2 + (2\xi\gamma)^2}} \tag{4}$$

As γ tends to zero, the expression for the sensitivity can be simplified as the static sensitivity, S_I, is independent of the applied frequency, and thus S_I can be rewritten as

$$S_I = \frac{(1 - p_e)m\lambda_B}{L_f(K_f + K_s)} \tag{5}$$

In general, the sensitivity is a function of the frequency and in the design of an effective FBG-based accelerometer, the static sensitivity S_I, is of greatest importance because it is very close to the 'flat range' sensitivity. High sensitivity and low fluctuation over a flat frequency range is a key design goal, not only to improve the resolution of signal, but also to improve the response characteristics in the low frequency band. The relationship between the theoretical sensitivity and the resonant frequency has important significance for creating an optimum device design. The sensitivity S_I and the resonant frequency f_n normalized with respect to the ratio $R(K_s/K_f)$ as a function of L_f is shown in Fig. 2 for different masses. It can be seen that the stiffness ratio R has a major influence on the sensitivity in the low frequency band, and as the frequency increases, the ratio R has a smaller influence on the sensitivity. As $K_f = E_f d^2/4L_f$, the sensitivity is a function of the length of the fiber, where the shorter the fiber length used, the higher is the sensitivity. At the same time, FBG-based
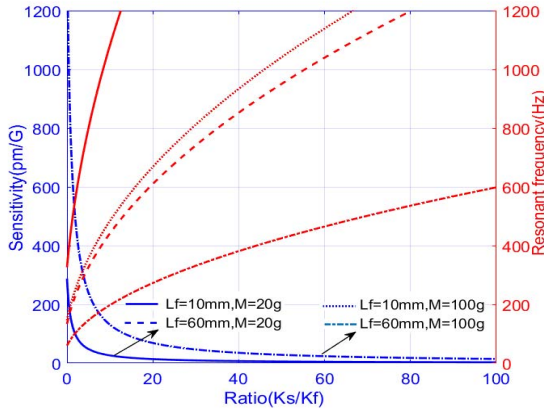
Fig. 2. Theoretical relationship between the sensitivity and resonant frequency with different stiffness ratios, R, and mass ($E_f = 7.2 \times 10^{10}$ P_a, d=0.125 mm).

Fig. 4. The relation between sensitivity and frequency, $E_d = 1.35 \times 10^{11}$ P_a, $L_f = 10$ mm, $E_f = 7.2 \times 10^{10}$ P_a, d= 0.125 mm.
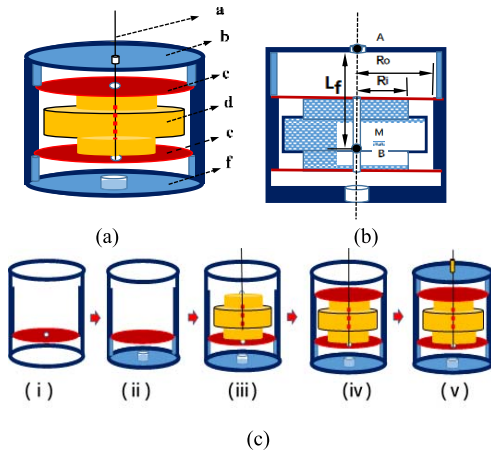

Fig. 3. Schematic of the FBG accelerometer designs. (a) Structural diagram where a is fiber, b is head cover, c is up diaphram, d is interial mass, e is low diaphram, f is base. (b) Cross-sectional view where Ro is outside radius, Ri is inside radius, Lf is the distance between poin A. (c) Schematic of the fabrication procedure for the device (i) to (v).

accelerometers with different lengths, L_f, of the fiber used and the same stiffness ratio, R, may have a similar sensitivity and resonant frequency, which then can be optimized. The maximum sensitivity that can be achieved is 1000pm/G – but the resonant frequency drops sharply below 50Hz. For the low frequency band (<100Hz), the length of fiber, has a significant influence on the resonant frequency (which cannot be ignored over this range, but it can more readily be ignored in the higher frequency range (>500Hz)).

B. Design and Optimization

The structure and fabrication issues for the optimization of the sensor system are shown schematically in Fig. 3. The inertial cylinder mass used is clamped between the two diaphragms, and is characterized by a thick middle and a thin end, with a through-hole is located at the central axis. A FBG is fixed between point A of the head cover and point B of the mass, as shown, this allowing the overall size of the device potentially to be reduced and thus the sensor to be more compact. When the sensor is subjected to acceleration along
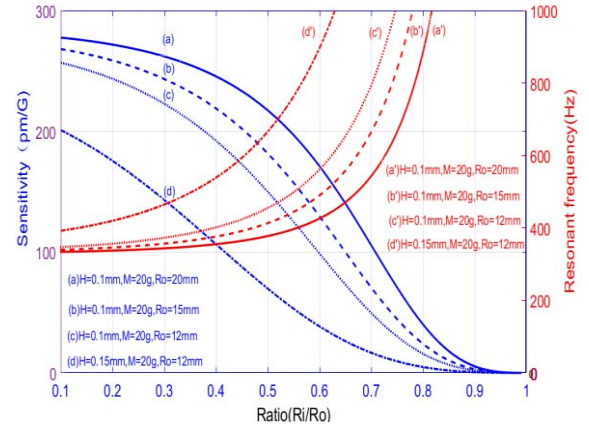
main axis, the inertial force induces a normal displacement of the diaphragms, resulting in a wavelength shift of the FBG. From the familiar principles of structural mechanics, the stiffness of the structure can be expressed as [24], [26]:

$$K_s = \frac{8\pi E_d H^3}{3\beta(1-\mu)R_o{}^2} \tag{6}$$

$$\beta = 1 - (\frac{R_i}{R_o})^2 - 4(\frac{R_i}{R_o})^2 (\ln \frac{R_i}{R_o})^2 / (1 - \frac{R_i{}^2}{R_o{}^2}) \tag{7}$$

where E_d, H, R_i, R_o, μ are the Young modulus, the thickness, the inside radius, the external radius and Possion's ratio respectively for the diaphragm. Combined with the Eq.3, Eq.5 and Eq.6, the sensitivity S_I and resonant frequency S_I can be expressed as is shown in Eq.8 and Eq.9 respectively.

$$S_I = \frac{3\lambda_B(1-P_e)}{L_f[\frac{8\pi E_d H^3}{3\beta(1-\mu)R_o{}^2} + \frac{E_f d^2}{4L_f}]}M \tag{8}$$

$$f_n = \sqrt{\frac{8\pi E_d H^3}{3M\beta(1-\mu)R_o{}^2} + \frac{E_f d^2}{4ML_f}} \tag{9}$$

The sensitivity S_I and the resonant frequency f_n, normalized with respect to the value of R_o as function of ratio R_i/R_o is plotted in Fig. 4 for different values of diaphragm thickness. Their relationship is in inversely proportional, as would be expected. The key issue is improving the overall performance, rather than just improving the sensitivity or resonant frequency alone and thus it is necessary to introduce a criterion for reflecting the integrated performance, for ease of evaluation and cross-comparison. Thus, a 'figure of merit' is proposed, where the concept of the product of the sensitivity and the resonant frequency (PSRF) is so defined, and this can be used as a basis for optimizing the performance. This PSRF-based 'figure of merit' will reflect the integrated performance of the sensor, as the higher the PSRF, the greater balancing range of sensitivity and the resonant frequency, the better the performance of the device. Thus, it is a simple, yet effective basis for optimizing the sensitivity along a constant frequency band, while at the same time, it provides comparability between different accelerometer designs. The PSRF thus
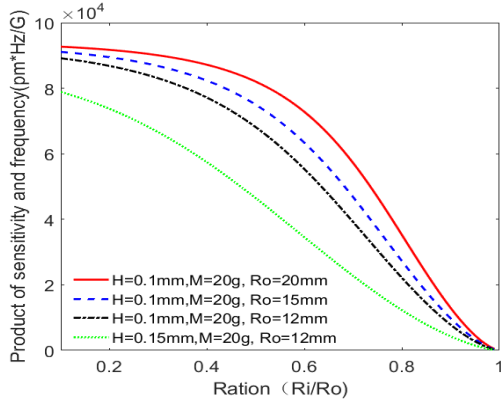
Fig. 5. The Product of sensitivity and resonant frequency.

TABLE I
PARAMETERS USED IN THE ACCELEROMETER MODELING

Symbol	Quantity	Value
E_d	Young's modulus of the diaphragm	1.35×10^{11} P$_a$
μ	Poisson's ratio of diaphragm	0.3
P_e	effective elastic-optical coefficient	0.22
R_i	radius of cylinder mass	6×10^{-3} m
R_o	radius of diaphragm	1.2×10^{-3} m
M	effective mass	20×10^{-3} kg
H	thickness of diaphragm	1×10^{-4} m
E_f	Young's modulus of the fiber	7.2×10^{10} P$_a$
L	Length of fiber between A and B	10×10^{-3} m
d	Diameter of fiber	1.25×10^{-4} m

can be expressed by Eq.8 and Eq.9, normalized with respect to the radius R_o and the thickness H as a function of the ratio R_i/R_o and this is plotted in Fig. 5. It can be seen that the PSRF decreases with increasing ratio (R_i/R_o), as generally when the ratio increases, the rate of sensitivity decrease is greater than the rate of frequency increase, and the smaller the ratio (R_i/R_o), the lower is the resonance frequency. As the ratio (R_i/R_o) rises from 0.1 to 0.5, the PSRF drops slowly, following which it decreases sharply when the ratio is >0.5. That is to say for best performance, the ratio (R_i/R_o) should not be too large and an optimum value exists. Thus for the low-frequencies experienced in oil/gas seismic exploration (where the range is typically up to 160Hz), to make sure the 'flat operational range' to being three times the working frequency. Combined with the relationship between the sensitivity and the resonant frequency, the core parameter R_i/R_o is then given by the value 0.5 and the other key parameters are as given in Table 1, where the theoretical sensitivity is 150.0pm/G, and the theoretical resonant frequency is ~454.0Hz, yielding a corresponding PSRF figure of merit of 6.8×10^4 pmHz/G.

III. EXPERIMENT AND DISCUSSION

The experimental setup used in this work is shown in Fig. 6, where the FBG accelerometer is fixed to a vibration table and a commercial piezoelectric accelerometer is used for cross-calibration. The FBG Interrogator (Type sm130 from Micron Optics, USA) with a wavelength reproducibility of 1 pm,
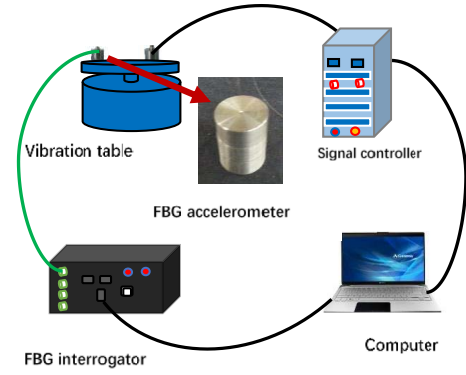

Fig. 6. Experimental setup of the system.

a scan frequency of 1 kHz and a wavelength range of 80 nm is used. In the experiment, the ambient temperature is recorded as 26 °C - but the effect of the temperature on the wavelength recorded is small (equivalent to <1Hz), over the time of the measurement was taken, any temperature effect can be ignored. In addition to this, the main factors that affect the temperature range are prestress (corresponding to ~1.15 nm), encapsulating adhesive (353ND), shell (aluminum alloy) diaphragm (QBe2), all of which are considered comprehensively. The theoretical temperature range considered is from −20 °C to 60 °C, but it is extremely difficult to change the temperature while measuring the acceleration in the experiment in the set up used. As a result, the extent of the temperature measurement range has not been experimentally determined in this work, but could represent a future investigation.

A. Linear Responsivity

Linear responsivity is an important characteristic of an accelerometer, defined as the relationship between the output wavelength and the applied acceleration. In the experiment carried out, the applied acceleration is sinusoidal in form, where the peak amplitude of the sinusoidal is given in units of G (where 1 G = 10.0 m/s^2) and the corresponding output signal is the wavelength of the FBG (it is also a harmonic oscillation, where the amplitude of the harmonic oscillation is the response to the applied acceleration). Experimental results obtained show that the accelerometer presents an extremely linear response, seen in Fig. 7, for a 100Hz and 160Hz harmonic oscillation output of the FBG accelerometer, and yielding a consequent sensitivity of 152.2pm/G for 160Hz. Fig. 8 shows the wavelength response in the time domain (where the harmonic oscillation output for the different accelerations at 100Hz and 160Hz are shown).

B. Amplitude-Frequency Characteristic

The amplitude-frequency characteristic of an accelerometer is an important feature that is distinctive from other static sensors. In essence, it reflects the relationship between the sensitivity and applied frequency. The theoretical analysis of the sensitivity indicates that this parameter increases as the frequency increases, reaching a maximum at the resonant frequency, and then starts to decay again beyond
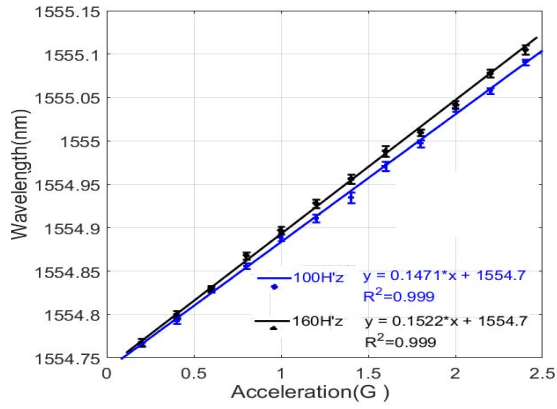
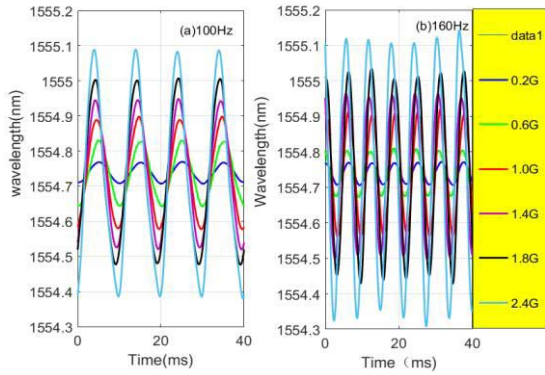Fig. 7.   Linear response of the accelerometer at 100Hz and 160 Hz.

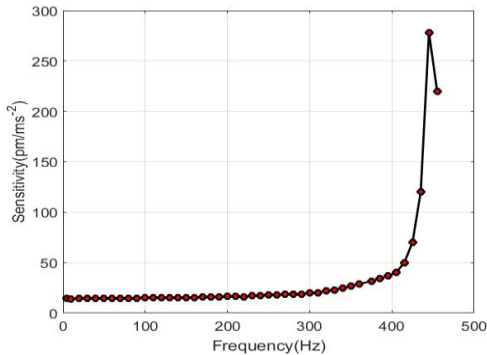Fig. 8.   Response in the time domain at 100Hz and 160 Hz.

Fig. 9.   Amplitude-frequency curve of the FBG accelerometer.

Fig. 10.   Shock response in the time domain.

Fig. 11.   FFT of the shock response (Figure 10).

that resonant frequency. In order to investigate further the amplitude-frequency characteristic of the FBG accelerometer design, the amplitude of the input signal is fixed at 0.1G, while the frequency of the applied signal is varied from 5 to 455 Hz. The amplitude-frequency response of the accelerometer that results is shown in Fig. 9, illustrating that the sensor has a broad flat response. In particular, what is important is that the low frequency range extends below 5Hz and with the approximate resonant frequency at 445 Hz, this offers a valuable characteristic for the device. The FBG Interrogator used (Type sm130) has a scan frequency of 1 kHz, setting a limit on the higher frequency signals that can be obtained. In order to obtain more accurate resonant frequency data, the Fast Fourier Transform (FFT) method has been adopted,
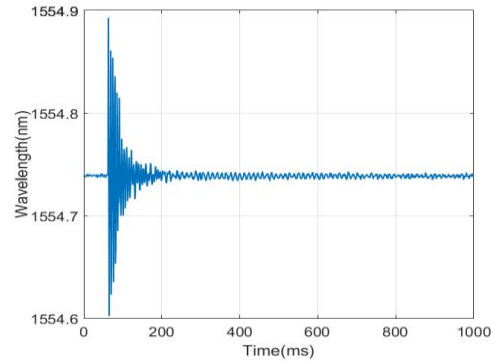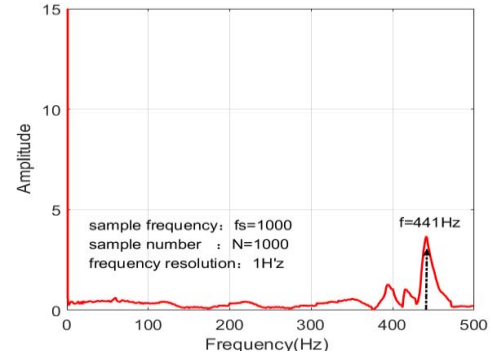
by using a manual impulse signal. The Fig. 10 shows the impulse signal in the time domain, while Fig. 11 shows the results of applying the fast Fourier transform (FFT) that results. The figure of 441Hz, obtained by this method is more reliable than that obtained previously (445Hz). Measurement results thus obtained agree well (within experimental error) with the theoretical resonant frequency calculated to be ~454Hz. In addition to this, the sensor presents a damped oscillation response. In practice, a damping fluid element has not been included to minimize the complexity of the sensor, with damping mainly due to the nature of the structure and the encapsulation.

C. Cross-Sensitivity

The accelerometer is a 'vector' sensor, and thus for a single freedom degree accelerometer, it is a problem for the designer to reduce the cross-axis sensitivity while at the same time enhancing the main-axis sensitivity–the smaller the cross sensitivity, the better the measurement result. In the experiment carried out, the excitation signal remained at 1 G, while the frequency of excitation signal increased from 5 to 300 Hz and the signals are applied to the main-axis and the 90 degree cross-axis. Fig. 12 shows the wavelength shift of the signals observed for the main-axis and cross-axis indicating that along the direction of the main-axis, the average of the peak wavelength shift is ~159pm, while the corresponding wavelength shift for the cross-axis is very small, at ~5.7pm (and thus the cross-axis sensitivity is <3.6% of that of the main-axis). This important result shows that the FBG-based accelerometer design considered has a strong resistance to interference to off-axis effects.
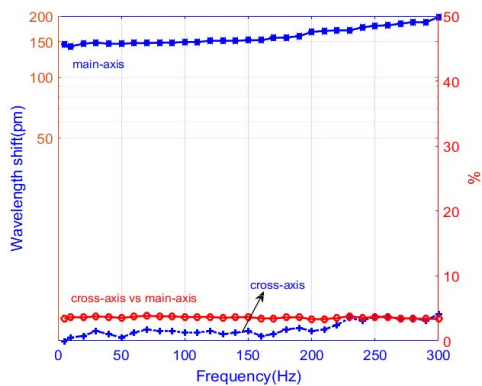
Fig. 12. The cross-sensitivity and main-sensitivity where the acceleration is 1G.
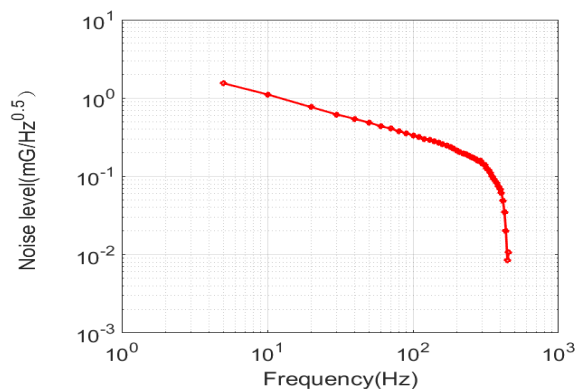

Fig. 13. Noise level in different frequency bands.

TABLE II
QUANTITATIVE COMPARISON OF PERFORMANCE OF THE REPORTED SCHEMES

PSRF / Reference	Data from literature [reference number]
PSRF<2.0×10^4	[8] [10-11] [13] [15-16] [20] [21-23] [26]
2.0×10^4<PSRF<5.0×10^4	[9] [12] [14] [17] [18-19] [24-25] [27] [29]
5.0×10^4<PSRF<6.5×10^4	[28]
PSRF>6.5×10^4	This study: **6.8×10^4**

D. Noise Level

The noise level is an important parameter for all kinds of accelerometer systems, as it reflects the ability of the device to detect weak signals over different frequency bands in practical applications. For this FBG accelerometer system, the equivalent noise over different bands was first measured and combined with the resolution ratio, allowing the noise level shown in Fig. 13 to be obtained. This is given by 0.26mG/Hz$^{0.5}$ over the 160Hz frequency band.

IV. CONCLUSION

A theoretical model has been developed, showing the high sensitivity of a FBG accelerometer designed. Based on the results of a model analyzed, a high-performance FBG accelerometer was developed, optimized and its performance discussed. The concept of a 'figure of merit', the product of sensitivity and frequency (PSRF) is introduced to allow a simple means of evaluation of the overall performance. Through appropriate theoretical modeling to allow the optimization of the design, the work undertaken has shown the following key features. Firstly, an effective theoretical model illustrating the high sensitivity of the FBG-based accelerometer design has been established and the theoretical relationship between the limit of the sensitivity and the resonant frequency has been proposed, this being dependent on the stiffness ratio. This is significant in improving performance and facilitating the miniaturization of the FBG accelerometer design. Secondly, the concept of the 'figure of merit', the PSRF, is introduced for comparison of the optimized overall performance, where the larger the PSRF, the closer the sensitivity is to the extreme limit of the theoretical model. Thus, under the conditions of the same frequency band, the larger the PSRF, the better the performance. Thirdly, the FBG accelerometer provides a broad frequency range of operation from 5 to 300 Hz, where the corresponding sensitivity ranges from 145.0 to 198.0 pm/G. An excellent feature is the low cross-axis sensitivity, which is less than 3.6% of the main-axis sensitivity. Thus, such a design is a good candidate for use in 'low frequency' oil and gas seismic exploration, and the theoretical analysis used provides an excellent deign framework giving confidence in the FBG-based accelerometer design that has been developed. The performance of the FBG-based device discussed in this work compares well with those considered in the literature, as can be seen from Table II, which summarizes performance data from a number of previously reported devices. The generic model based on double-point encapsulation which has been established shows a sensitivity obtained which is greater than other sensor designs when viewing this within a similar frequency band [17], [19], [21]. The 'figure of merit' (PSRF) used is much higher than that for the other sensors, data on which has been taken from the literature [8]–[29]. Data summarized in Table II thus show key features of the performance and sensitivity achieved in light of published work.

REFERENCES

[1] P. F. da C. Antunes *et al.*, "Optical fiber accelerometer system for structural dynamic monitoring," *IEEE Sensors J.*, vol. 9, no. 11, pp. 1347–1354, Nov. 2009.
[2] P. Antunes, R. Travanca, H. Varum, and P. André, "Dynamic monitoring of mobile telecommunication towers exposed to natural loading with a FBG biaxial accelerometer," in *Proc. 16th OECC*, Kaohsiung, Taiwan, Jul. 2011, pp. 591–592.
[3] Y. Zhang *et al.*, "Fiber Bragg grating sensors for seismic wave detection," *Proc. SPIE*, vol. 5855, pp. 1008–1011, Aug. 2005.
[4] X. Qiao, Z. Shao, W. Bao, and Q. Rong, "Fiber Bragg grating sensors for the oil industry," *Sensors*, vol. 17, p. 429, Feb. 2017.
[5] A. Laudati *et al.*, "A fiber optic Bragg grating seismic sensor," *Proc. SPIE*, vol. 6619, pp. 66191C-1–66191C-4, Jul. 2007.
[6] X. L. Zhang *et al.*, "Reliable high sensitivity FBG geophone for low frequency seismic acquisition," *Measurement*, vol. 129, pp. 62–67, Dec. 2018.
[7] I. Talebinejad, C. Fischer, and F. Ansar, "Low frequency fiber optic accelerometer for civil structural health monitoring," *Proc. SPIE*, Apr. 2009, vol. 7294, Art. no. 729412.
[8] M. D. Todd, G. A. Johnson, B. A. Althouse, and S. T. Vohra, "Flexural beam-based fiber Bragg grating accelerometer," *IEEE Photon. Technol. Lett.*, vol. 10, no. 11, pp. 1605–1607, Nov. 1998.
[9] A. Mita and I. Yokoi, "Fiber Bragg grating accelerometer for structural health monitoring," in *Proc. 5th Int. Conf. Motion Vib. Control*, 2000, pp. 4–8.
[10] Y. Wong *et al.*, "A robust and compact fiber Bragg grating vibration sensor for seismic measurement," *IEEE Sensors J.*, vol. 12, no. 4, pp. 800–804, Apr. 2011.

[11] M. M. Khan, N. Panwar, R. Dhawan, "Modified cantilever beam shaped FBG based accelerometer with self temperature compensation," *Sens. Actuators A, Phys.*, vol. 205, pp. 79–85, Jan. 2014.

[12] D. Feng *et al.*, "A fiber Bragg grating accelerometer based on a hybridization of cantilever beam," *IEEE Sensors J.*, vol. 15, no. 3, pp. 1532–1537, Mar. 2015.

[13] N. Basumallick, P. Biswas, K. Dasgupta, and S. Bandyopadhyay, "Design optimization of fiber Bragg grating accelerometer for maximum sensitivity," *Sens. Actuators A, Phys.*, vol. 194, pp. 31–39, May 2013.

[14] X. Zhang, Q. Rong, H. Sun, S. Yang, L. Yuan, and M. Hu, "Low-frequency fiber Bragg grating accelerometer based on a double-semicircle cantilever," *Opt. Fiber Technol.*, vol. 20, pp. 190–193, Jun. 2014.

[15] J. Zhang *et al.*, "Flextensional fiber Bragg grating-based accelerometer for low frequency vibration measurement," *Chin. Opt. Lett.*, vol. 9, no. 9, Sep. 2011, Art. no. 090607.

[16] Q. Liu, Z. Jia, H. Fu, D. Yu, H. Gao, and X. Qiao, "Double cantilever beams accelerometer using short fiber Bragg grating for eliminating chirp," *IEEE Sensors J.*, vol. 16, pp. 6611–6615, Sep. 2016.

[17] Y. Yu, Z. Meng, and H. Luo, "Study on fiber Bragg grating vibrating sensors with symmetry push-pull configuration," *Semicond. Optoelectron.*, vol. 32, no. 1, pp. 118–122, 2011.

[18] Q.-P. Liu, X.-G. Qiao, J.-L. Zhao, Z.-A. Jia, H.-W. Fu, and H. Gao, "Study on fiber Bragg grating acceleration sensing based on elastic tube," *J. Optoelectron. Laser*, vol. 23, no. 7, pp. 1227–1232, Mar. 2012.

[19] J. Wang, Y. Zeng, C. Lin, Z. Hu, G. Peng, and Y. Hu, "A miniaturized FBG accelerometer based on a thin polyurethane shell," *IEEE Sensors J.*, vol. 16, no. 15, pp. 1210–1216, Mar. 2016.

[20] Y. S. Zhang *et al.*, "Study on a fiber Bragg grating accelerometer based on compliant cylinder," *Opt. Fiber Technol.*, vol. 26, pp. 229–233, Dec. 2015.

[21] N. Gutiérrez, P. Galvín, and F. Lasagni, "Low weight additive manufacturing FBG accelerometer: Design, characterization and testing," *Measurement*, vol. 117, pp. 295–303, Mar. 2018.

[22] X. Wang, Y. Guo, L. Xiong, and H. Wu, "High-frequency optical fiber Bragg grating accelerometer," *IEEE Sensors J.*, vol. 18, no. 12, pp. 4954–4960, Jun. 2018.

[23] M. S. Müller, T. C. Buck, and A. W. Koch, "Fiber Bragg grating-based acceleration sensor," in *Proc. Int. Symp. Optomechatronic Technol.*, Istanbul, Turkey, 2009, pp. 127–132.

[24] X.-C. Li, S. Liu, W.-T. Zhang, F.-X. Zhang, F. Li, and Y.-L. Liu, "Study on low-frequency characteristic of double-diaphragm fiber Bragg grating geophone," *J. Optoelectron. Laser*, vol. 21, no. 4, pp. 529–532, Apr. 2010.

[25] X. D. Luo, X. G. Qiao, Z. A. Jia, M. Shao, and D. Q. Feng, "The experimentation of fiber Bragg grating geophone," *Prog. Geophys.*, vol. 27, no. 3, pp. 1203–1206, Mar. 2012.

[26] Q. P. Liu, X. G. Qiao, J. L. Zhao, Z. A. Jia, H. Gao, and M. Shao, "Novel fiber Bragg grating accelerometer based on diaphragm," *IEEE Sensors J.*, vol. 12, no. 10, pp. 3000–3004, Oct. 2012.

[27] Q. Liu, X. Qiao, Z. Jia, H. Fu, H. Gao, and D. Yu, "Large frequency range and high sensitivity fiber Bragg grating accelerometer based on double diaphragms," *IEEE Sensors J.*, vol. 14, no. 5, pp. 1499–1504, May 2014.

[28] L. Qiu, L. Liang, D. Li, and G. Xu, "Theoretical and experimental study on FBG accelerometer based on multi-flexible hinge mechanism," *Opt. Fiber Technol.*, vol. 38, pp. 142–146, Nov. 2017.

[29] F. Liu, Y. Dai, J. M. Karanja, and M. Yang, "A low frequency FBG accelerometer with symmetrical bended spring plates," *Sensors*, vol. 17, no. 1, p. 206, Jan. 2017.

[30] K. O. Hill and G. Meltz, "Fiber Bragg grating technology fundamentals and overview," *J. Lightw. Technol.*, vol. 15, no. 8, pp. 1263–1276, Aug. 1997.

Qinpeng Liu was born in Anhui, China, in 1977. He received the Ph.D. degree from the School of Northwestern Polytechnical University in 2015, major in optical engineering. His current research interests are mainly focused on optical fiber sensing and their applications.

Xue He was born in Shanxi, China, in 1994. She is currently pursuing the M.S. degree with the Key Laboratory on Photoelectric Oil-Gas Logging and Detecting, Ministry of Education, Xi'an Shiyou University.

Xueguang Qiao was born in Shanxi, China, in 1955. He received the Ph.D. degree in science from the Xi'an Institute of Optics and Fine Mechanics, Chinese Academy of Sciences, in 1998, major in optics. His current research interests include optoelectronic technology, optical fiber communication, and sensing.

Tong Sun received the B.E., M.E., and D.Eng. degrees from the Department of Precision Instrumentation, Harbin Institute of Technology, Harbin, China, in 1990, 1993, and 1998, respectively, and the Ph.D. degree in applied physics from the City, University of London, London, U.K., in 1999.

She was an Assistant Professor with Nanyang Technological University, Singapore, from 2000 to 2001, before she rejoined the City, University of London in 2001, as a Lecturer. Subsequently, she was promoted as a Senior Lecturer in 2003, a Reader in 2006, and a Professor in 2008 at the City, University of London, where she is currently the Director of the Research Centre of Sensors and Instrumentation and is leading a research team focused on developing a range of optical fiber sensors for a variety of industrial applications, including structural condition monitoring, early fire detection, homeland security, process monitoring, food quality, and environmental monitoring. She has been working closely with partners across disciplines from academia and industry, both in the U.K. and overseas. She has authored or co-authored some 230 scientific and technical papers. Dr. Sun is a member of the Institute of Physics and a Fellow of the Institution of Engineering and Technology. She is a Chartered Physicist and a Chartered Engineer in U.K.

Kenneth T. V. Grattan received the B.Sc. (Hons.) degree in physics from Queens University Belfast, Belfast, U.K., in 1974, the Ph.D. degree in laser physics in the use of laser-probe techniques for measurements on potential new dye laser systems, and the D.Sc. degree from the City, University of London, London, U.K., in 1992, for his work in sensor systems.

In 1978, he became a Research Fellow with the Imperial College of Science and Technology, to work on advanced photolytic drivers for novel laser systems. In 1983, he joined the City, University of London, as a new blood Lecturer in Physics, being appointed as a Professor of Measurement and Instrumentation, and the Head of the Department of Electrical, Electronic and Information Engineering in 1991. He was the President of the Institute of Measurement and Control in 2000. He was the Dean of the School of Engineering and Mathematical Sciences and the School of Informatics, City, University of London, from 2008 to 2012. He was appointed as the Dean of the City Graduate School in 2012. He has authored more than 700 publications in major international journals and a similar number at international conferences. His research interests include the use of fiber optic and optical systems in the measurement of a range of physical and chemical parameters for industrial applications. He is the Co-Editor of a five volume topical series on Optical Fiber Sensor Technology.

Dr. Grattan was a recipient of the Callendar Medal and the Honeywell Prize of the Institute of Measurement and Control. He was elected as a Fellow of the Royal Academy of Engineering in 2008.